ELSEVIER

Tectonophysics 308 (1999) 237–248

TECTONOPHYSICS

www.elsevier.com/locate/tecto

Microseismic activity and seismotectonics of Heraklion Area (central Crete Island, Greece)

N. Delibasis [a], M. Ziazia [a], N. Voulgaris [a,*], T. Papadopoulos [a], G. Stavrakakis [b], D. Papanastassiou [b], G. Drakatos [b]

[a] *Geophysics–Geothermy Division, Department of Geology, University of Athens, Athens GR-15784, Greece*
[b] *Institute of Geodynamics, National Observatory of Athens, Athens GR-11810, Greece*

Received 2 February 1998; accepted 28 July 1998

Abstract

A seismological network of 10 portable analogue stations was installed in the area of Heraklion (central Crete) from September to December 1995. During this period, more than 1000 events were recorded by at least 4 stations with magnitudes ranging from 0.5 to 4.6 and depths up to 70 km. Analysis of 336 well located events revealed high seismic activity. In the onshore area seismicity is shallow (<20 km) and concentrated along the eastern margin of the Heraklion Basin and in the Messara graben to the south. Seismicity decreases rapidly from east to west, with practically no events located along the western boundary of Heraklion Basin. Epicenter distribution indicates that microseismicity is closely associated to the tectonics of the region. Significant seismic activity was also observed in the southern offshore area, restricted north of the Hellenic Trench and related to the subduction process. The determination of different types of focal mechanisms in the area indicates that the investigated region is characterized by complex tectonics related to the southward subduction of the African plate and the northward extension of the Aegean lithosphere.

Keywords: Greece; Hellenic Trench; Crete; seismotectonics

1. Introduction

Located at the southernmost extremity of the Hellenic Island Arc (Fig. 1), the island of Crete is considered as an area of important tectonic deformation and high seismic activity, resulting from the collision between the Eurasian and African plates and the subduction of the latter under the former (McKenzie, 1972, 1978; Papazachos, 1973; Angelier, 1979; Papadopoulos et al., 1986; Spakman et al., 1988; Drakatos and Drakopoulos, 1991; Papazachos et al., 1995; Alessandrini et al., 1997; Drakatos et al., 1997). As a result of this complex tectonic deformation several damaging earthquakes have occurred since historical times (Papazachos and Papazachou, 1997).

The region is one of intense seismicity, most of which occurs in a belt of about 100 km wide that roughly follows the bathymetry of the Hellenic Trench to the south of the island (McKenzie, 1978). The northern part of the island (Sea of Crete) forms

* Corresponding author. Tel./Fax: +30 1 7247445; E-mail: nvoulgar@atlas.uoa.gr

0040-1951/99/$ – see front matter
PII: S0040-1951(99)00076-1

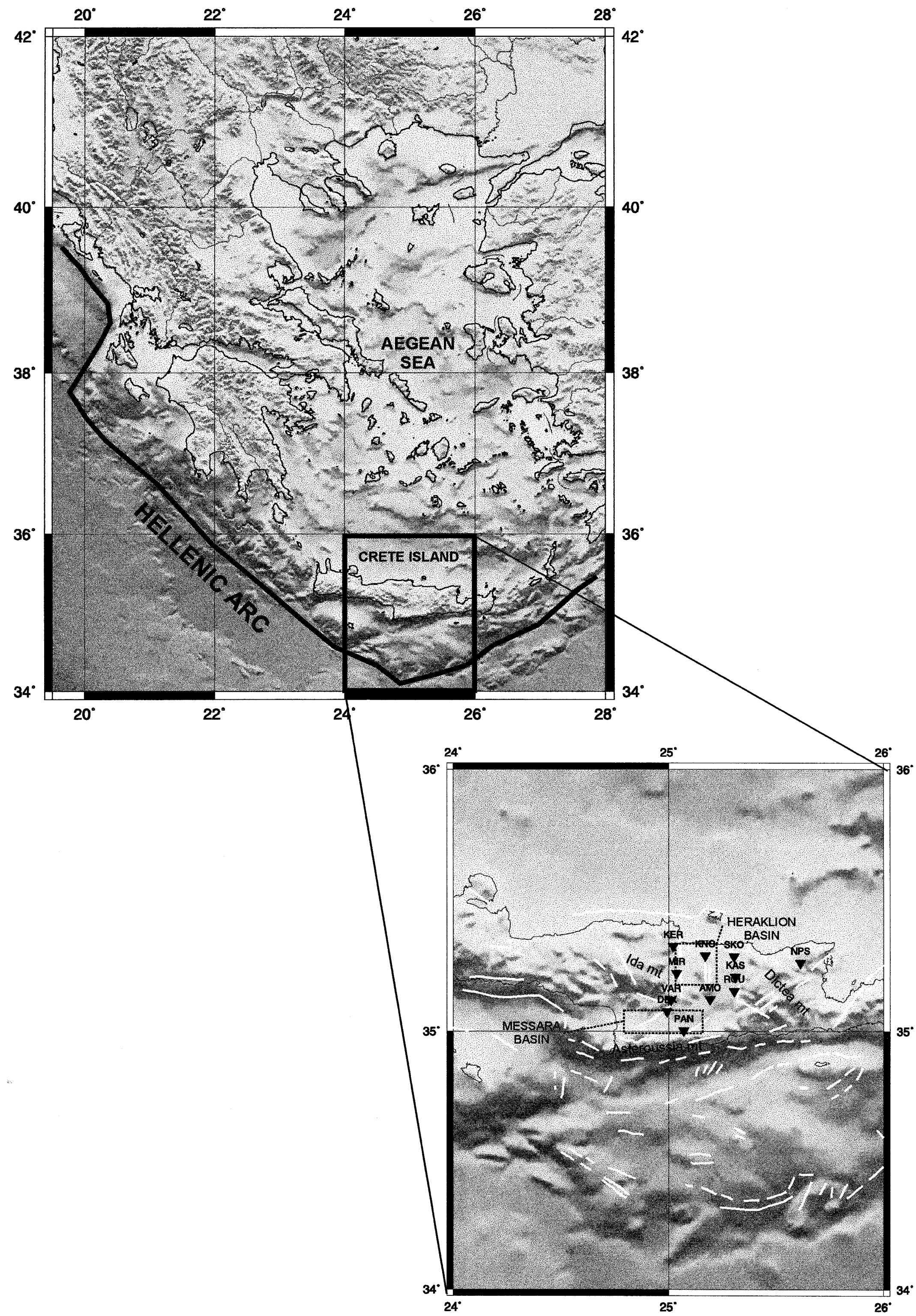
20°
22°
24°
26°
28°
42°
40°
38°
36°
34°
AEGEAN SEA
HELLENIC ARC
CRETE ISLAND
25°
35°
HERAKLION BASIN
MESSARA BASIN
Ida mt
Dictea mt
KER
KNO
SKO
NPS
MIR
KAS
VAR
AMO
PAN

part of the Aegean extensional province and is relatively aseismic, although studies on land and sea reveal neogene normal faulting that continues as far south as the inner wall of the Hellenic Trench (Angelier et al., 1982). Thus, intermediate depth seismicity in Crete Island is related to the north–south convergence between the African and European plates, while most of the shallow events are probably associated with crustal extension within the Aegean (Taymaz et al., 1990). Hence, both extensional and compressional stresses are present in the area, resulting in complex fault tectonics characterized by important horizontal and vertical movements (Comninakis and Papazachos, 1980; Delibasis et al., 1982). The focal mechanisms of shallow earthquakes ($h < 60$ km) indicate an extensional stress field trending NE–SW and NW–SE, in accordance with the observed normal fault scarps (Fig. 1) in the area (Armijo et al., 1992). Moreover, according to tectonic observations (Angelier, 1979), extension trends E–W in the western part, NE–SW in the central area and NNW–SSE in the eastern part of Crete. Furthermore, the E–W extension of the western part is also supported by the results of field experiments (De Chabalier et al., 1992 and Hatzfeld et al., 1993).

In 1995, in the framework of a microzonation project, the Institute of Geodynamics (National Observatory of Athens, NOA) and the University of Athens (Geophysics–Geothermy Division) installed a network of ten portable seismological stations in the central Crete area, which complemented two permanent stations belonging to the NOA. The portable stations operated for a time period of three months. During the summer of 1988, Hatzfeld et al. (1993) installed a network of portable seismological stations in the islands of the southern Aegean Sea. However, no stations were deployed in the central Crete area.

Therefore, this study is a first attempt to investigate in detail the seismotectonics of this region, characterized by a rather complex pattern of uplifted massifs, where various elements of alpine formations have been identified, and subsident basins filled with unconformable neogene and quaternary sediments. The average width of the uplifted blocks is 30 km. This is close to the thickness of the crust and suggests that the horst and graben structure does not affect the mantle (Angelier et al., 1982).

Two tectonic grabens dominate the central Crete region on shore, the Heraklion to the north and the Messara in the southwest (Fig. 1). The Heraklion graben is bounded by the Ida mountain in the west and the Dictea mountain to the east, along the Malevizi and Kasteli fault zones, respectively (Angelier, 1979; Fytrolakis, 1980; Delibasis et al., 1982). Both fault zones have an average NNE–SSW direction, with the Malevizi fault zone being more distinctly emphasized by the topography of the Ida mountain. The Messara graben is bounded by the Ida mountain in the north and the Asteroussia range to the south along two E–W-trending fault zones. A third important graben structure can be identified in the offshore area south of the island, defined by a series of E–W-trending faults (Angelier, 1979).

2. Data acquisition and processing

On June 1995, ten portable seismographs were installed in the Heraklion area (Fig. 1). Additionally, in order to improve the accuracy of the earthquake parameters, recordings of two permanent stations on Crete Island have been used. To obtain the best possible determination of epicenters, an adequate velocity model for the region should be used. Therefore, the minimum 1D model technique (Kissling et al., 1994, 1995) was adopted. According to this technique, the arrival time of a seismic wave is a non-linear function of the location of the stations (s), the focal depth and the origin time (h) and the velocity model (m), that is:

$$t_{\text{obs}} = f(s, h, m). \tag{1}$$

In this relation, only the location of the stations and the arrival times are known. Hence, to solve the problem, it is necessary to determine an initial velocity model. Then, the forward problem can be solved

Fig. 1. Location map of the investigated region. The solid triangles in the enlarged map of the area correspond to seismological station locations. White solid lines represent the main faults in the area according to Angelier (1979). The location of the Messara and Heraklion Basins is also indicated.

and the calculated arrival times and their residuals can be estimated. Using the inversion method, the corrections of the velocity model and earthquake parameters are calculated, in order to minimize the time residuals. The procedure is repeated until the overall RMS value remains almost constant. During the final stage, station corrections are also computed in order to minimize location uncertainties.

To obtain better results, it is necessary that the above-mentioned procedure is repeated, starting from different initial velocity models. For the definition of initial velocity models, three different velocity models proposed by Papazachos et al. (1966), Makris (1977) and Hatzfeld et al. (1993) have been reviewed. The final velocity model obtained after data processing is shown in Fig. 2. In the same figure, the velocity model derived by De Chabalier et al. (1992) for western Crete is also shown. The large number of available phase data allowed the relative refinement of the model used by De Chabalier et al. (1992).

In the minimum 1D velocity model (Fig. 2) obtained, three main velocity discontinuities can be observed at depths of 6, 16 and 30 km with mean velocities of 5.2, 6.2, 6.7, and 7.7 km/s, respectively. In addition, a V_p/V_s ratio of 1.78 was calculated,

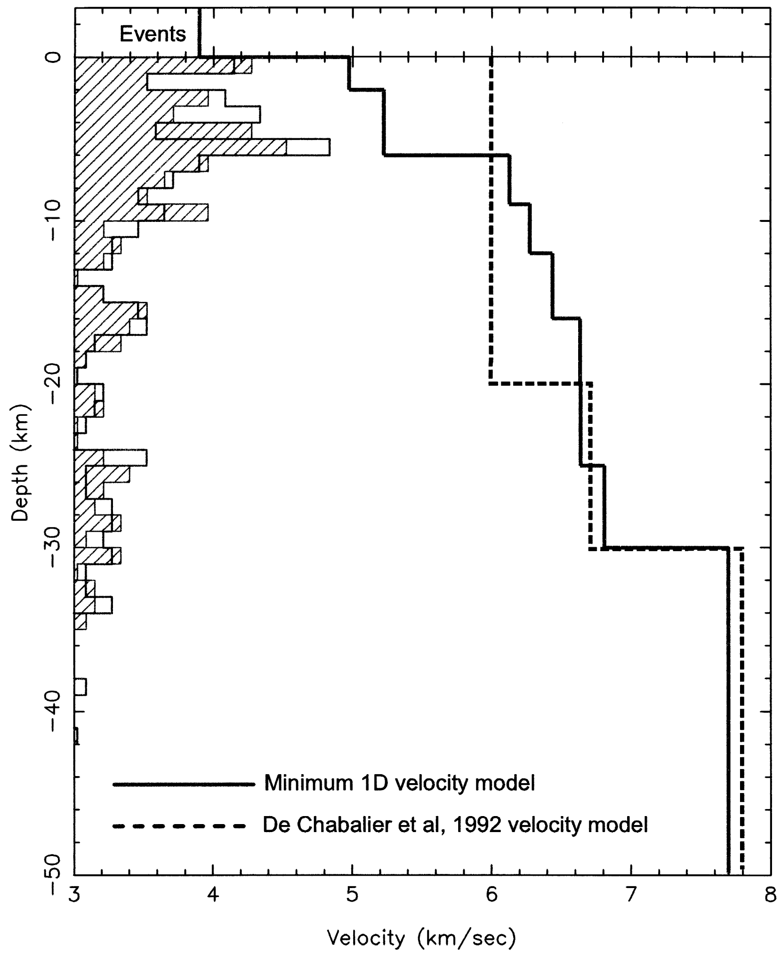

Fig. 2. The minimum 1D velocity model used for epicenter location in this study compared to the velocity model used by De Chabalier et al. (1992). The depth distribution of earthquakes with respect to the initial (solid line) and final (shaded area) velocity model is also shown.

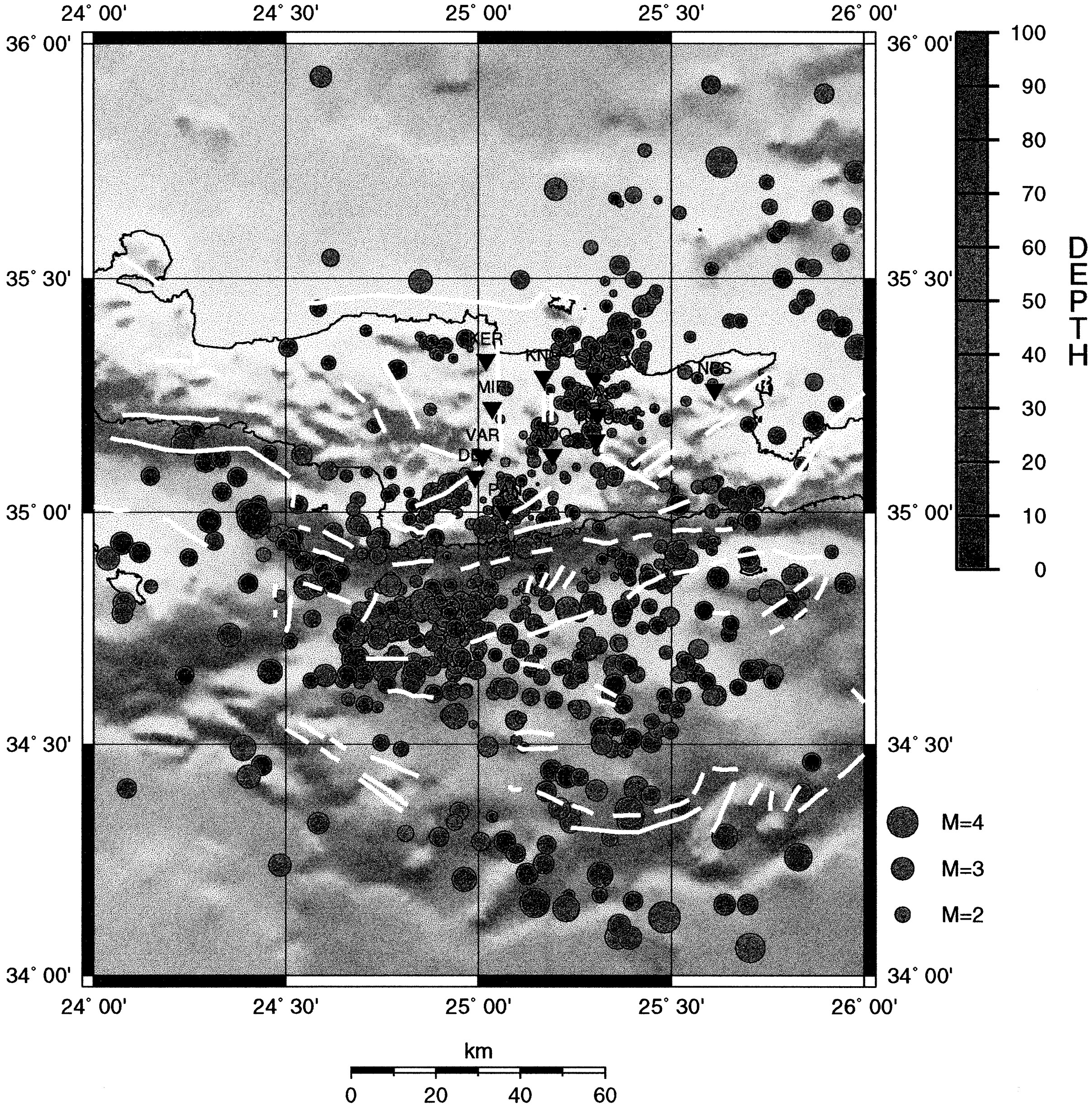

Fig. 3. Epicenter distribution of all located (845) events recorded during a 3-month period in central Crete.

which confirms the relatively high values of 1.79 and 1.80 computed by Hatzfeld et al. (1990) and De Chabalier et al. (1992), respectively. Finally, the depth distribution of earthquakes with respect to the final velocity model is more even, compared to the one corresponding to the initial model (Fig. 2).

Regarding the magnitude calculation, the following relation was used:

$$M_{\mathrm{L}} = a \log T + bD + C, \tag{2}$$

where T is the time duration of records (in seconds), D is the epicentral distance, and a, b, C are constants.

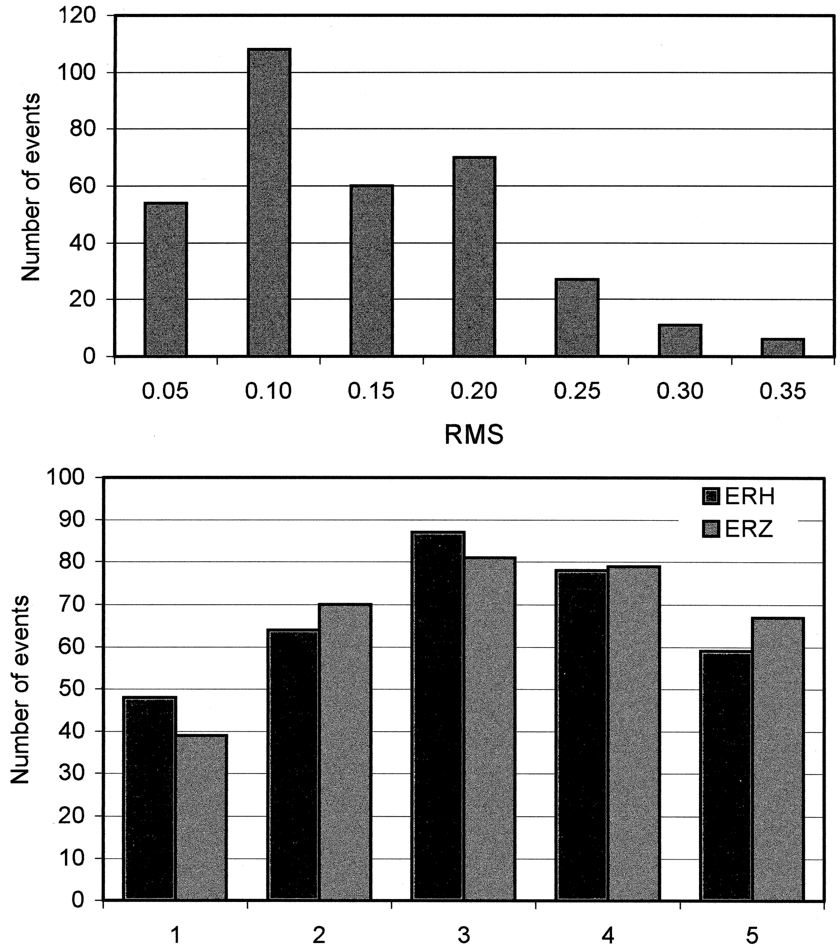

Fig. 4. Epicenter determination uncertainties (RMS, ERH and ERZ) for the 336 better-located events.

The values of a, b, C are taken from similar studies concerning the Greek area (Kiratzi and Papazachos, 1984; Papanastassiou, 1989). The formula used was:

$$M_{\mathrm{L}} = 2.31 \log T + 0.0012D + 0.73. \quad (3)$$

3. Epicenter distribution — seismotectonics

During the three-month period that the network was in operation, more than 1000 micro-earthquakes have been recorded. In Fig. 3, the epicenters of the 845 located events, having at least four P and one S phases, are shown. Their magnitudes range from 0.5 to 4.6 and their depths between 1 and 70 km. The number of earthquakes is significantly high compared to the events recorded during previous experiments in Crete Island (De Chabalier et al., 1992; Hatzfeld et al., 1993). High seismic activity is observed in the offshore region southward of the island in the subduction zone area, while in the northern offshore area the activity is significantly lower.

From the initial data set, considering as reliable values RMS $<$ 0.4 and ERH, ERZ $<$ 6 (Fig. 4), 336 better located events were selected (Fig. 5). In the onshore area, seismicity is mainly distributed in the eastern and southern part of the investigated region. Especially, a cluster trending NNE–SSW is located in the northeastern margin of Heraklion Basin. Two more clusters, trending NE–SW and N–S, are located in the northwestern and central

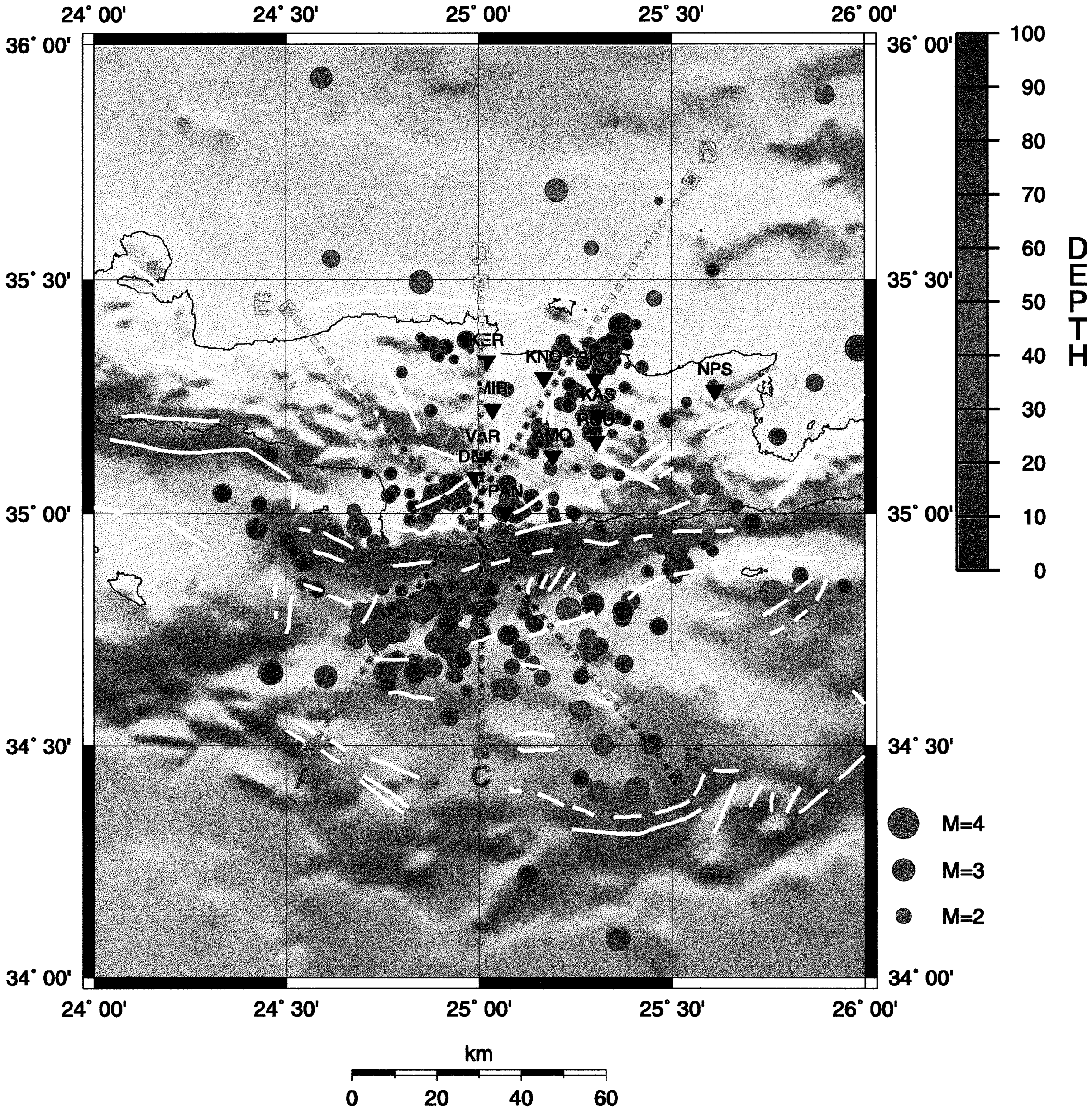

Fig. 5. Epicenter distribution of the better-located (336) earthquakes. The directions of three cross-sections used in this study are also plotted.

part of the Messara Basin, respectively. A smaller cluster appears west of the Heraklion Basin, to the north of Ida mountain. The majority of these events is limited to depths shallower than 20 km (Fig. 6, cross-sections A–B, C–D and E–F). Relatively high seismic activity can be observed in the offshore area south of the island, following the E–W trend of regional faulting (Angelier, 1979). Activity along this zone is extended up to 30 km (Fig. 6) and should not be confused with that of the subduction zone along the Hellenic Trench, which is characterized by deeper seismic activity (Fig. 6, cross-section A–B).

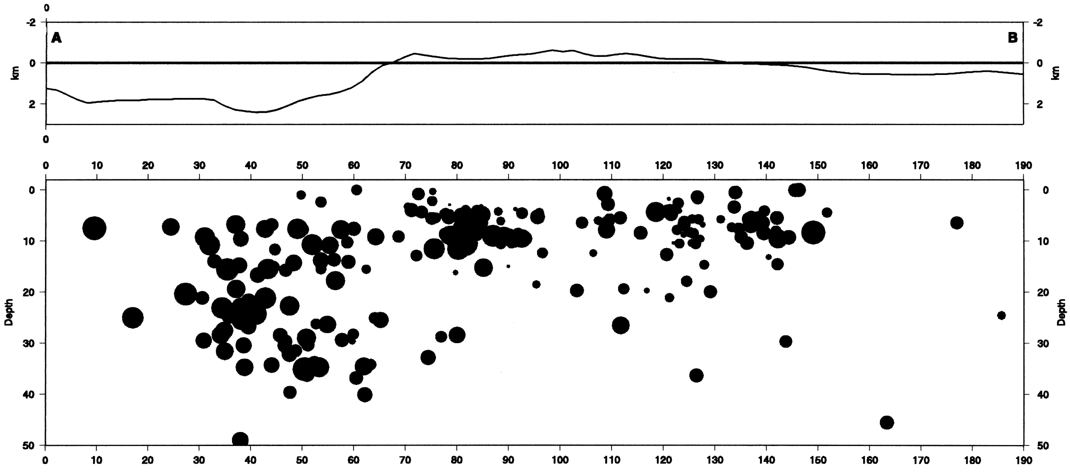
A
B
km
Depth

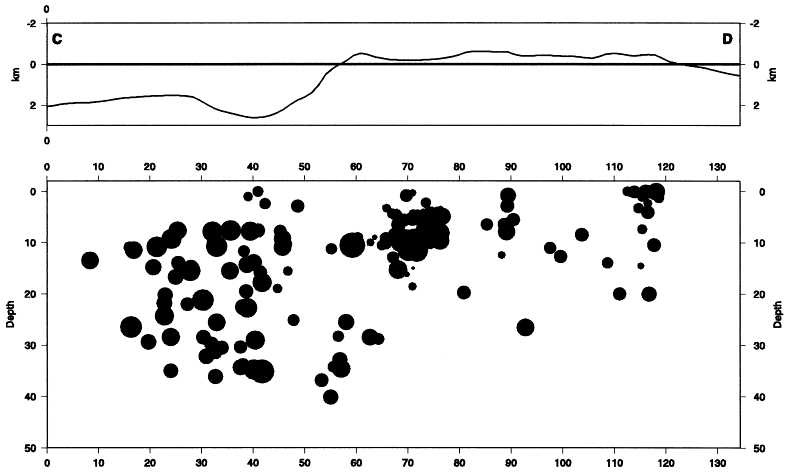
C
D
km
Depth

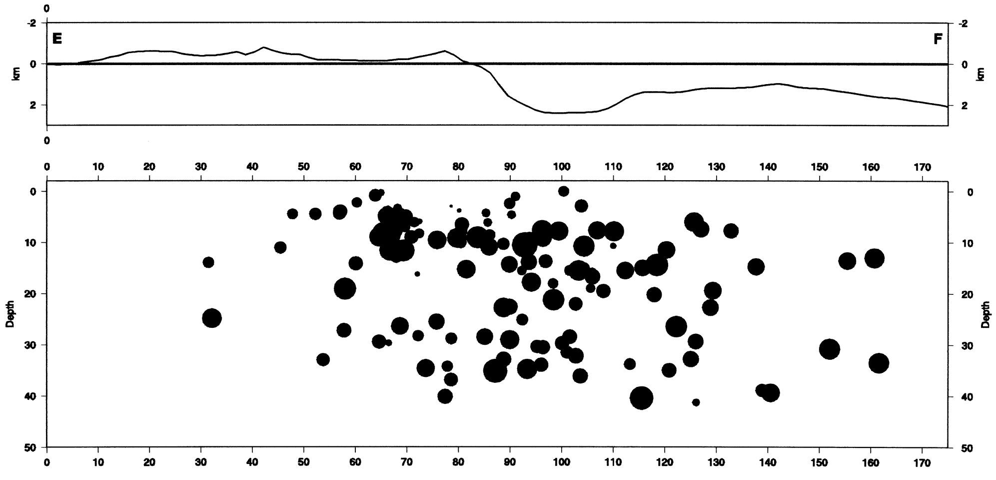
E
F
km
Depth

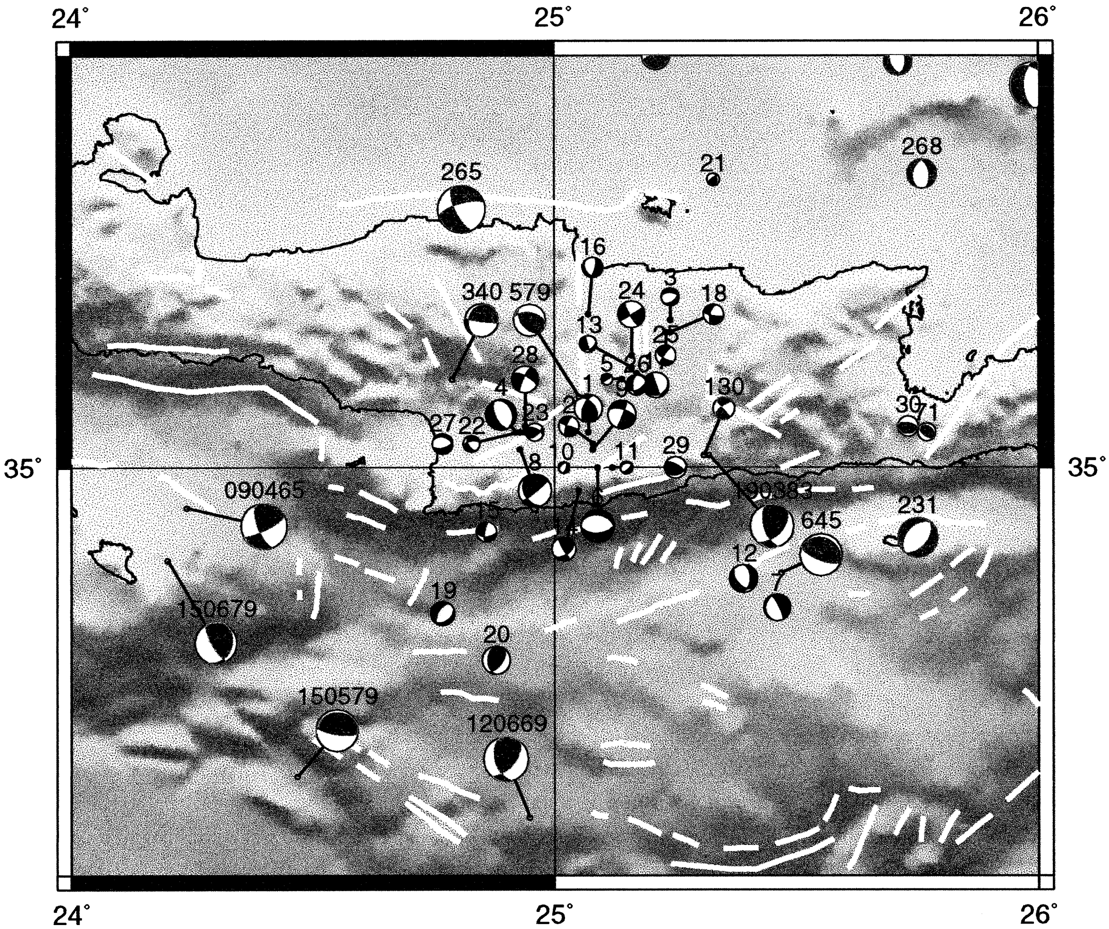

Fig. 7. Well-constrained focal mechanisms calculated for the Central Crete Area (black-and-white spheres). Focal mechanisms from Taymaz et al. (1990) and Hatzfeld et al. (1993) are also shown as dark-gray-and-white and light-gray-and-white spheres, respectively.

Using P-wave polarity data the focal mechanisms of 102 events were calculated, with 61 of them indicating normal and 41 reverse motion. The calculation was based on the computer program designed by Reasenberg and Oppenheimer (1985). Since the uncertainty in the mechanism is mostly a function of the distribution of polarities on the focal sphere, selection of better-constrained solutions was performed, accepting those with at least three populated quadrants and a minimum of 8 P-wave polarities. This procedure resulted in a total of 29 focal mechanisms (Fig. 7). As can be seen from this figure, most of the well-constrained mechanisms correspond to events located onshore, within the boundaries of the local seismological network. Their parameters are listed in Table 1. Moreover, selected focal mechanisms computed by Taymaz et al. (1990) for large earthquakes in the area and by Hatzfeld et al. (1993) for the events recorded during the 1988 experiment are also shown in Fig. 7.

Fig. 6. Epicenter distribution cross-sections along the directions A–B, C–D and E–F depicted in Fig. 5. The vertical exaggeration of the corresponding topographic profile plotted above each section is 1 : 4.

Table 1
Parameters of the focal mechanisms

No.	Date	Time	Lat. (°N)	Long. (°E)	Depth	Magnitude	Plane 1			Plane 2		*P*-axis		*T*-axis	
							Az	Dip	Rake	Az	Dip	Az	Dip	Az	Dip
1	950907	16:03	35.06	25.07	9.6	2.4	320	50	41	201	60	263	6	164	53
2	950908	0:37	35.04	25.08	9.0	1.8	290	90	180	200	70	63	13	156	13
3	951008	2:53	35.25	25.24	6.3	1.6	55	45	−120	274	52	245	68	345	3
4	951029	19:01	35.06	24.92	8.1	2.7	335	30	−90	155	60	65	75	245	15
5	951031	11:29	35.15	25.14	12.4	1.0	60	85	90	240	5	150	40	330	50
6	951113	7:38	35.00	25.09	9.1	2.9	85	55	−100	282	36	320	77	182	9
7	951121	1:23	34.76	25.46	7.3	2.3	185	15	−60	334	77	234	57	70	31
8	950903	17:03	35.03	24.93	11.6	2.9	150	35	11	51	84	113	30	353	40
9	950907	6:29	35.03	25.08	9.2	2.5	20	85	−150	287	60	247	24	149	16
10	950911	21:32	35.00	25.02	4.9	0.0	15	55	−109	227	39	234	71	119	7
11	950912	13:48	35.00	25.12	4.3	1.1	45	60	−110	261	35	274	68	149	12
12	950915	13:33	34.81	25.39	23.3	2.4	140	50	−119	1	48	342	67	250	1
13	950925	14:08	35.17	25.16	5.8	1.5	65	35	−10	163	84	41	40	281	30
14	951007	5:37	34.96	25.05	28.5	2.1	150	85	40	55	50	276	23	20	30
15	951014	18:30	34.89	24.86	36.9	1.8	190	75	−139	87	51	56	38	314	14
16	951015	19:23	35.26	25.07	8.5	1.8	140	30	−139	13	71	315	57	85	22
17	951020	14:09	35.16	25.17	7.9	2.2	70	20	0	340	90	51	41	268	41
18	951026	18:55	35.23	25.24	4.8	1.8	100	80	−30	195	60	53	28	151	13
19	951027	0:45	34.75	24.77	24.1	2.1	55	35	−70	211	57	84	73	310	11
20	951027	19:46	34.67	24.88	24.3	2.5	180	40	60	37	56	110	8	357	69
21	951028	19:20	35.49	25.33	18.3	1.1	350	45	31	237	69	299	14	192	48
22	951029	19:04	35.06	24.93	4.1	1.4	260	60	−140	147	56	115	48	22	2
23	951029	20:15	35.06	24.94	5.4	1.6	50	60	40	297	56	172	2	265	48
24	951102	14:11	35.19	25.16	26.6	2.3	60	90	−180	150	80	14	7	105	7
25	951105	8:03	35.23	25.23	4.2	1.8	120	65	−11	214	80	79	24	344	10
26	951109	15:39	35.16	25.17	2.9	1.8	65	50	−40	183	60	40	53	301	6
27	951120	6:13	35.04	24.77	4.0	1.8	75	60	−110	291	35	304	68	179	12
28	951126	1:18	35.07	24.94	4.9	2.3	205	80	−20	298	70	160	21	253	6
29	951207	20:04	35.00	25.25	5.3	1.9	75	30	50	299	67	13	19	240	62

4. Discussion and conclusions

During the operation of the local network in central Crete Island, a large number of earthquakes were recorded. This indicates that the investigated region is characterized by significant seismic activity. This observation is consistent with the intense tectonic deformation outlined along this part of the Hellenic Arc (Angelier, 1979).

In the onshore area, the epicenter distribution shows that most of the seismic activity is concentrated along the eastern margin of the Heraklion Basin and in the Messara graben to the south (Figs. 3 and 5). Seismicity decreases rapidly from east to west, with practically no events located along the western boundary of the Heraklion Basin. These observations are in agreement with the results presented by Hatzfeld et al. (1993) and the tectonic features recorded by Angelier (1979) and Fytrolakis (1980). Comparison of epicenter locations with the main tectonic features derived from Angelier (1979) reveals that most of these features are related to microseismic activity. This is especially evident in the Messara graben as well as at the eastern margin of the Heraklion graben (Figs. 3 and 5). In addition, the cluster located east of Heraklion city, trending NNE–SSW, suggests the existence of a tectonic feature. The relatively shallow ($<$20 km) character of the onshore seismic activity and its relation to the local faulting are also evident from the cross-sections of Fig. 6. The fault plane solutions in the onshore area indicate both normal and reverse motion and in some cases significant horizontal slip component.

The spatial distribution of well-located events

(Fig. 5) indicates significant seismic activity in the southern offshore area. The seismicity in this region appears to be restricted to the north of the Hellenic Trench, as was also observed during the experiment of Hatzfeld et al. (1993), and is related to the subduction of the African plate under the Aegean lithosphere. However, two regions of seismic activity should be distinguished. The first one is restricted to relatively shallow depths (Fig. 6, cross-sections A–B, C–D) along the southern coastline of Crete Island, associated with the offshore graben structure defined by E–W-trending faults (Angelier, 1979). Additionally, the calculated fault plane solutions in this area indicate normal faulting (Fig. 7). Therefore, this activity appears to be related to tectonic deformation along the front of the overriding Aegean plate and should not be confused with the deeper seismicity of the second region, which is associated with the African slab. As can be seen from cross-sections A–B and C–D, the geometry of the subducting plate appears to be well defined down to a depth of 50 km. The focal mechanisms from large events in this region (Taymaz et al., 1990) indicate reverse faulting (Fig. 7), as expected in a typical subduction area.

The overview of seismic activity in the onshore and offshore areas indicates a complex seismotectonic regime. This could be the result of the existence of both extensional and compressional stress fields in the area (Taymaz et al., 1990), resulting from the convergence of the African and European plates as well as from the extension within the Aegean Basin.

Acknowledgements

The authors are grateful to Dr. D. Hatzfeld and an anonymous reviewer for their constructive comments and suggestions. This study was partially supported by the Research Project under contract no. 654, funded by the General Secretariat for Research and Technology (Greece).

References

Alessandrini, B., Beranzoli, L., Falcone, C., Mele, F., Drakatos, G., Karantonis, G., Stavrakakis, G., 1997. Back arcs basins and P-wave crustal velocity in the Ionian and Aegean regions. Geophys. Res. Lett. 24 (5), 527–530.

Angelier, J., 1979. Néotectonique de l'arc Egéen. Soc. Geol. du Nord, 3.

Angelier, J., Lyberis, N., Le Pichon, X., Barrier, E., Huchon, P., 1982. The tectonic development of the Hellenic arc and the sea of Crete: a synthesis. Tectonophysics 86, 159–196.

Armijo, R., Lyon-Caen, H., Papanastassiou, D., 1992. East–west extension and holocene normal faults scraps in the Hellenic arc. Geology 20, 491–494.

Comninakis, P.E., Papazachos, B.C., 1980. Space and time distribution of the intermediate focal depth earthquakes in the Hellenic arc. Tectonophysics 70, T35–T37.

De Chabalier, J.B., Lyon-Caen, H., Zollo, A., Deschamps, A., Bernard, P., Hatzfeld, D., 1992. A detailed analysis of microearthquakes in western Crete from digital three-components seismograms. Geophys. J. Int. 110, 347–360.

Delibassis N., Drakopoulos, J., Fytrolakis, N., Katsikatsos, G., Makropoulos, K., Zamani, A., 1982. Seismotectonic investigation of Crete Island and the adjacent areas. Int. Symposium on the Hellenic arc and the Trench (H.E.A.T.), Vol. 1, Athens.

Drakatos, G., Drakopoulos, J., 1991. 3-D velocity structure beneath the crust and upper mantle of the Aegean sea region. Pure Appl. Geophys. 135, 401–420.

Drakatos, G., Karantonis, G., Stavrakakis, G., 1997. P-wave crustal tomography of Greece with use of an accurate two-point ray tracer. Ann. Geofis. XL (1), 25–36.

Fytrolakis, N., 1980. The Geological Structure of Crete. Nat. Tech. Univ. Athens, Special Publication.

Hatzfeld, D., Pedotti, G., Hatzidimitriou, P., Makropoulos, K., 1990. The strain pattern in the western Hellenic arc deduced from a microearthquake survey. Geophys. J. Int. 101, 181–202.

Hatzfeld, D., Besnard, M., Makropoulos, K., Hatzidimitriou, P., 1993. Microearthquake seismicity and fault planes solutions in the southern Aegean and its geodynamic implications. Geophys. J. Int. 115, 799–818.

Kiratzi, A.A., Papazachos, B.C., 1984. Magnitude scales for earthquakes in Greece. Bull. Seism. Soc. Am. 74 (3), 969–985.

Kissling, E., Ellsworth, W.L., Eberhart-Phillips, D., Kradolfer, U., 1994. Initial reference models in local earthquake tomography. J. Geophys. Res. 99 (B10), 19635–19646.

Kissling, E., Solarino, S., Cattaneo, M., 1995. Improved seismic velocity reference model from local earthquake data in Northwestern Italy. Terra Nova 7, 528–534.

Makris, J., 1977. Geophysical investigations of Hellenides. Hamburger Geophys. Einzelschr. 34, Univ. Hamburg.

McKenzie, D.P., 1972. Activity tectonics of the Mediterranean region. Geophys. J. R. Astron. Soc. 30, 109–185.

McKenzie, D.P., 1978. Active tectonics of the Alpine–Himalayan belt: the Aegean sea and surrounding regions. Geophys. J. R. Astron. Soc. 55, 217–254.

Papadopoulos, G.A., Kondopoulou, D., Leventakis, G.-A., Pavlides, S., 1986. Seismotectonics of the Aegean region. Tectonophysics 124, 67–84.

Papanastassiou, D., 1989. Detectability, locatability and accuracy of focal parameters determination by the seismographic network of the NOA. Ph.D. thesis, Univ. of Athens, 225 pp. (in Greek).

Papazachos, B.C., 1973. Distribution of seismic foci in the Mediterranean and surrounding area and its tectonic implications. Geophys. J. R. Astron. Soc. 33, 419–428.

Papazachos, B.C., Comninakis, P.E., Drakopoulos, J., 1966. Preliminary results of an investigation of crustal structure in southeastern Europe. Bull. Seism. Soc. Am. 56 (6), 1241–1268.

Papazachos, B. and C. Papazachou, 1997. The Earthquakes of Greece. Ziti Publ., Thessaloniki, Greece.

Papazachos, C.B., Hatzidimitriou, P.M., Panagiotopoulos, D.G., Tsokas, G.N., 1995. Tomography of the crust and upper mantle in southeast Europe. J. Geophys. Res. 100 (B7), 12405–12422.

Reasenberg, P.A., Oppenheimer, D., 1985. FPFIT, FPPLOT, FPPAGE: Fortran computer programs for calculating and displaying earthquake fault-plane solutions. USGS Open File Rep. No. 85-739.

Spakman, W., Wortel, M.J.R., Vlaar, N.J., 1988. The Hellenic subduction zone: a tomographic image and its dynamic implications. Geophys. Res. Lett. 15, 60–63.

Taymaz, T., Jackson, J.A., Westway, R., 1990. Earthquake mechanisms in the Hellenic Trench near Crete. Geophys. J. Int. 102, 695–732.